Published for SISSA by Springer

Received: April 15, 2011
Revised: July 6, 2011
Accepted: July 15, 2011
Published: July 26, 2011

A parton shower for High Energy Jets[1]

Jeppe R. Andersen,[a] **Leif Lönnblad**[b,c] **and Jennifer M. Smillie**[d]

[a] *CP3-Origins, University of Southern Denmark, Campusvej 55, DK-5230 Odense M, Denmark*
[b] *CERN Theory Department, CH-1211 Geneva, Switzerland*
[c] *Dept. of Astronomy and Theoretical Physics, Lund University, Sölvegatan 14A, SE-223 63 Lund, Sweden*
[d] *School of Physics and Astronomy, University of Edinburgh, Mayfield Road, EH9 3JZ Edinburgh, UK*

E-mail: andersen@cp3.sdu.dk, Leif.Lonnblad@thep.lu.se, j.m.smillie@ed.ac.uk

Abstract: We present a method to match the multi-parton states generated by the High Energy Jets Monte Carlo with parton showers generated by the Ariadne program using the colour dipole model. The High Energy Jets program already includes a full resummation of soft divergences. Hence, in the matching it is important that the corresponding divergences in the parton shower are subtracted, keeping only the collinear parts. We present a novel, shower-independent method for achieving this, enabling us to generate fully exclusive and hadronized events with multiple hard jets, in hadronic collisions. We discuss in detail the arising description of the soft, collinear and hard regions by examples in pure QCD jet-production.

Keywords: Jets, Phenomenological Models, Hadronic Colliders, QCD

ArXiv ePrint: 1104.1316

[1] Work supported in parts by the EU Marie Curie RTN MCnet (MRTN-CT-2006-035606), the Swedish research council (contracts 621-2008-4252 and 621-2009-4076) and the UK Science and Technology Facilities Council (STFC).

doi:10.1007/JHEP07(2011)110

JHEP07(2011)110

Contents

1 Introduction

The CERN Large Hadron Collider is testing not only several suggested extensions of the Standard Model, but is simultaneously testing the theoretical description of particle collisions within the Standard Model. With the increased energy at the LHC over earlier colliders, the accurate theoretical description of several observables will necessitate the inclusion of several additional jets of hardness similar to that of the relevant lowest-order process being studied.

The all-order perturbative description included in the general-purpose Monte Carlo programs [1–4] relies on properties of soft- and collinear radiation from the lowest-order hard process, and therefore underestimates the amount of radiation of similar hardness. The shower-description of radiative corrections can be corrected above a chosen merging-scale with the full tree-level matrix elements with, e.g., the CKKW(-L) [5, 6] or MLM [7] approach. The multiplicity, to which the tree-level matrix elements are required to be evaluated, will depend on the chosen merging scale. A low merging scale will correct the parton shower in much of phase space, but the multiplicity to which the tree-level matrix elements must be evaluated is then very large (and in practice the maximum multiplicity is limited).

Several alternative approaches have been developed in order to respond to the need for the description of semi-hard emissions to all orders, not just those which can be reached by matching from the shower-formalism. Some of these approaches, like Cascade [8, 9] and ARIADNE [6], originate from the study of specific phase space regions at earlier colliders, where the semi-hard radiative corrections were already deemed relevant. In the formulation of Cascade, the semi-hard emissions are generated from the PDF-evolution according to

JHEP07(2011)110

the CCFM equation [10–13], while ARIADNE implements the *Colour Dipole Model* [14–17] of the evolutions of colour dipoles after the hard scattering.

The current study uses the new approach of *High Energy Jets* (*HEJ*) [18–20], which is built on standard collinear factorisation between hard scattering matrix elements and PDFs, but calculates the hard scattering matrix elements to all orders. This is achieved within an approximation, which becomes exact in the limit of large invariant mass between all particles. This is the exact opposite limit of collinear emissions. The close similarity between the formulation of the resummation in *HEJ* and the normal perturbative expansion of a fixed-order calculation allows for a simple procedure [20] for matching the *HEJ* resummation to full tree-level accuracy, similar to the merging of a parton shower and matrix elements in a CKKW-L or MLM merging procedure.

The multi-jet predictions from *HEJ* are in the form of partonic final states, with no collinear enhancement of radiation. While *HEJ* describes the jet count and topology, jet shapes are completely ignored. The jet cones are mostly empty, except for the single parton taking up all the jet momentum, not unlike the situation of a tree-level generator.

In order to arrive at a more realistic description of the final state of the particle scattering, first a resummation of the (soft[1] and) collinear emissions of a parton shower is necessary, in order to secondly add a hadronisation step. While the description of jet profiles within *HEJ* is not unlike the situation at tree-level, the challenge of matching the description to a shower is completely unlike that at tree-level solved in the approach of CKKW [5, 6], MLM [7] or VINCIA [21]. This is because *HEJ* is summing its own tower of real corrections to all orders and, on top of that, also includes the leading virtual corrections in the limit of hard, wide angle emissions. The challenge of matching *HEJ* with a shower is to avoid double counting between the two all-order approaches.

We will present a shower-independent subtraction algorithm for matching *HEJ* and a parton shower. Furthermore, this paper contains a study of the effects of the parton shower and hadronisation on the predictions arising from *HEJ*. This is obtained for an implementation of the specific evolution of the final state according to ARIADNE, with the string hadronisation as implemented in PYTHIA [22, 23]. In section 2 we present the ingredients of *HEJ* necessary for the further discussion, and in section 3 we do the same for ARIADNE. Section 4 presents the matching of the two all-order perturbative approaches. Section 5 discusses the impact of the addition of the shower and hadronisation on various classes of observables, both some very sensitive to the description of collinear radiation (the shower profile), and some which will turn out to be modified only slightly (e.g. vetos of hard jets). The addition of a parton shower on top of *HEJ* should extend the validity of the prediction to regions with a large ratio also of transverse scales.

Finally, in section 6 we present our conclusions and outline some future improvements of our matching procedure.

2 The High Energy Jets Monte Carlo

The *High Energy Jets (*HEJ*)* framework [18–20] provides a perturbative approximation to the hard scattering matrix elements to jet production to any order in the coupling, which

[1] We will in fact see later that much of the soft radiation is already resummed in *HEJ*.

JHEP07(2011)110

is exact in the limit of large invariant mass between all particles. The formalism is inspired by the high energy factorisation of matrix elements (as pioneered by BFKL [24–27]), in that only certain partonic configurations are described (namely those leading in the limit of large invariant mass between all partons, also denoted Multi-Regge Kinematics — *MRK*). Within the framework of BFKL, a number of kinematic approximations are applied in order to cast the cross section in the form of a two-dimensional integral equation. This also entails a number of approximations to the phase space. These approximations are avoided within *HEJ*. The advances in computing power allow the calculation of the cross section as an explicit integration over matrix elements of each multiplicity, with the inclusion of (an approximation to the) virtual corrections, and a simple organisation of the cancellation of IR singularities between real and virtual corrections. This allows for the construction of an approximation, which retains the logarithmic accuracy of the BFKL approach, but is more accurate when compared to the full QCD amplitudes in the phase space regions relevant for the LHC. The details are discussed in ref. [18–20]; here we will briefly repeat the discussion of the points which are necessary for constructing the matching to a parton shower.

The all-order treatment in *HEJ* starts with the approximation to the tree-level scattering amplitude for the scattering process with flavours $f_1 f_2 \to f_1 g \cdots g f_2$, where the final state particles are listed according to their rapidity, and f_1, f_2 can be quarks, anti-quarks or gluons. We will call these states *FKL*-configurations (Fadin-Kuraev-Lipatov [25]). The scattering amplitude is approximated at lowest order by the following expression [20]

$$\begin{aligned}\left|\overline{\mathcal{M}}^t_{f_1 f_2 \to f_1 g \ldots g f_2}\right|^2 &= \frac{1}{4\ (N_C^2-1)}\ \left\|S_{qQ\to qQ}\right\|^2 \\ &\cdot \left(g^2\ K_{f_1}\ \frac{1}{t_1}\right) \cdot \left(g^2\ K_{f_2}\ \frac{1}{t_{n-1}}\right) \\ &\cdot \prod_{i=1}^{n-2} \left(\frac{-g^2 C_A}{t_i t_{i+1}}\ V^\mu(q_i, q_{i+1}) V_\mu(q_i, q_{i+1})\right),\end{aligned} \tag{2.1}$$

where $\left\|S_{f_1 f_2 \to f_1 f_2}\right\|^2$ indicates the square of pure current-current scattering, and K_{f_1}, K_{f_2} are flavour-dependent colour-factors (which can depend also on the momentum of the particles of each flavour f_1, f_2, see ref. [20] for more details). The use of flavour-dependent colour factors allows one to display explicitly the complete factorisation at tree-level of all QCD processes $f_1 f_2 \to f_1 f_2$ into contractions of normal currents over a t-channel pole. $g^2 = 4\pi\alpha_s$ is the QCD coupling, and t_i is the square of the local t-channel momentum, $t = q_i^2$, $q_i = p_a - \sum_{j=1}^{i} p_j$, where p_a momentum of the incoming parton of negative z-momentum, and the momenta p_i of the outgoing partons are ordered with increasing rapidity.

The effective vertex for emissions of gluons takes the form [18]

$$\begin{aligned}V^\rho(q_i, q_{i+1}) = &-(q_i + q_{i+1})^\rho \\ &+ \frac{p_A^\rho}{2}\left(\frac{q_i^2}{p_{i+1}\cdot p_A} + \frac{p_{i+1}\cdot p_B}{p_A \cdot p_B} + \frac{p_{i+1}\cdot p_n}{p_A \cdot p_n}\right) + p_A \leftrightarrow p_1 \\ &- \frac{p_B^\rho}{2}\left(\frac{q_{i+1}^2}{p_{i+1}\cdot p_B} + \frac{p_{i+1}\cdot p_A}{p_B \cdot p_A} + \frac{p_{i+1}\cdot p_1}{p_B \cdot p_1}\right) - p_B \leftrightarrow p_n.\end{aligned} \tag{2.2}$$

JHEP07(2011)110

This form of the effective vertex is fully gauge invariant; the Ward Identity, $p_j \cdot V = 0$ ($j = 2, \ldots, n-1$) can easily be checked, and is valid for all momenta p_j (i.e. not just in the *MRK*-limit). This allows for a meaningful approximation to the scattering amplitude to be constructed.

The virtual corrections are approximated with the *Lipatov ansatz*[27] for the t-channel gluon propagators (see ref. [18] for more details). This is obtained by the simple replacement in eq. (2.1) of

$$\frac{1}{t_i} \;\to\; \frac{1}{t_i}\,\exp\left[\hat{\alpha}(q_i)(y_{i-1}-y_i)\right] \tag{2.3}$$

with

$$\hat{\alpha}(q_i) = -g^2\, C_A\, \frac{\Gamma(1-\varepsilon)}{(4\pi)^{2+\varepsilon}}\frac{2}{\varepsilon}\left(\mathbf{q}_i^2/\mu^2\right)^{\varepsilon}, \tag{2.4}$$

where $\hat{\alpha}$ is regulated in $D = 4 + 2\varepsilon$ dimensions and $\mathbf{q}_i^2$ is the Euclidean square of the transverse components of q_i. The cancellation of the poles in ε between the real and virtual corrections is organised with a mix of a subtraction and a phase space slicing (basically limiting the phase space region of the subtraction terms), such that the regulated matrix elements used in the resummation of *HEJ* are given by [20]

$$\begin{aligned}
\overline{\left|\mathcal{M}^{\mathrm{reg},f_1f_2\to f_1g\cdots gf_2}_{\mathrm{HEJ}}(\{p_i\})\right|}^2 &= \frac{1}{4\,(N_C^2-1)}\;\|S_{f_1f_2\to f_1f_2}\|^2 \\
&\cdot\left(g^2\,K_{f_1}\,\frac{1}{t_1}\right)\cdot\left(g^2\,K_{f_2}\,\frac{1}{t_{n-1}}\right) \\
&\cdot\prod_{i=1}^{n-2}\left(g^2C_A\,\left(\frac{-1}{t_it_{i+1}}V^{\mu}(q_i,q_{i+1})V_{\mu}(q_i,q_{i+1})-\frac{4}{\mathbf{p}_i^2}\,\theta\left(\mathbf{p}_i^2<\lambda^2\right)\right)\right) \\
&\cdot\prod_{j=1}^{n-1}\exp\left[\omega^0(q_j,\lambda)(y_{j-1}-y_j)\right], \\
\omega^0(q_j,\lambda) &= -\frac{\alpha_sC_A}{\pi}\log\frac{\mathbf{q}_j^2}{\lambda^2}.
\end{aligned} \tag{2.5}$$

The all-order dijet cross section is then simply calculated as the phase space integral over any number of gluon emissions from the initial scattering $f_1f_2 \to f_1f_2$. Matching to high-multiplicity tree-level matrix elements is obtained by reweighting the event with the ratio of the square of the tree-level matrix element (evaluated using MadGraph [28]) and the approximation to this in eq. (2.1), both evaluated on a set of momenta derived from the hard jets only (in order to reduce the multiplicity, and therefore not to exhaust the limited number of available full tree-level matrix elements too quickly). This procedure is

JHEP07(2011)110

summarised in the following formula

$$\sigma_{2j}^{\text{resum,match}} = \sum_{f_1,f_2} \sum_{n=2}^{\infty} \prod_{i=1}^{n} \left(\int_{p_{i\perp}=0}^{p_{i\perp}=\infty} \frac{\mathrm{d}^2\mathbf{p}_{i\perp}}{(2\pi)^3} \int \frac{\mathrm{d}y_i}{2} \right) \frac{\overline{|\mathcal{M}_{\text{HEJ}}^{f_1 f_2 \to f_1 g \cdots g f_2}(\{p_i\})|}^2}{\hat{s}^2}$$
$$\times \sum_m \mathcal{O}_{mj}^e(\{p_i\})\ w_{m-\text{jet}} \tag{2.6}$$
$$\times \quad x_a f_{A,f_1}(x_a, Q_a)\ x_2 f_{B,f_2}(x_b, Q_b)\ (2\pi)^4\ \delta^2\left(\sum_{i=1}^{n} \mathbf{p}_{i\perp} \right)\ \mathcal{O}_{2j}(\{p_i\}),$$

where n is the partonic multiplicity of the final state. The second line in eq. (2.6) describes the matching of *HEJ* to high-multiplicity tree-level by a reweighting of the exclusive m-jet rate projected with the operator $\mathcal{O}_{mj}^e$ with the ratios of the relevant tree-level matrix elements. The last line describes the inclusion of PDFs and the momentum-conserving delta-functional. We define the inclusive two-jet operator $\mathcal{O}_{2j}$ to return one if the final state contains at least two hard ($p_\perp > 35\,\text{GeV}$) jets; in the current study, we use the anti-kt algorithm with an $R = 0.6$, and the E-recombination scheme. Furthermore, we require that the extremal partons from HEJ are members of the extremal jets, in order to ensure that the partonic configuration matches the situation for which the *HEJ* resummation scheme was developed.

The partonic configurations not conforming to the ordering described above are included in *HEJ* by simply adding the contributions order-by-order (again using `MadGraph` [28]), but no all-order summation is performed of these non-*FKL* configurations. In the current study, we will focus on the *FKL*-configurations, since this is where special all-order attention is needed in order to avoid double counting in the subsequent shower. The non-FKL configurations could possibly be added to the combined *HEJ*+shower sample through e.g. a vetoed CKKW-L-procedure (vetoing any *FKL*-configuration which might arise).

The matching of *HEJ* to high-multiplicity tree-level accuracy is currently performed with up to four jets in the final state, limited by the time taken to evaluate the full expressions. Importantly, the description in *HEJ* goes beyond approximating leading-order high-multiplicity matrix elements. As discussed, the *Lipatov ansatz* [27] is used to give an approximation to the virtual corrections at all orders in addition. This resums to all-orders the leading logarithmic virtual corrections to the t-channel poles.

By construction, the *HEJ* framework therefore provides a description directed particularly at hard, wide-angle QCD radiation. The transverse momenta of gluons emitted in-between (in rapidity) the two extremal partons can take on any value, however the subtraction suppresses the contribution from emissions with a transverse momentum less than λ. We note that although eq. (2.5) contains the exponential of the logarithm of a momentum, it is not directly related to a Sudakov factor of a normal parton shower — firstly, the logarithm is not of the emitted momentum, secondly, the resummation is not formulated as a unitary evolution (i.e. of constant total cross section). In order to perform a matching to a parton shower, we have to *define* the relation between the emissions of *HEJ* and

JHEP07(2011)110

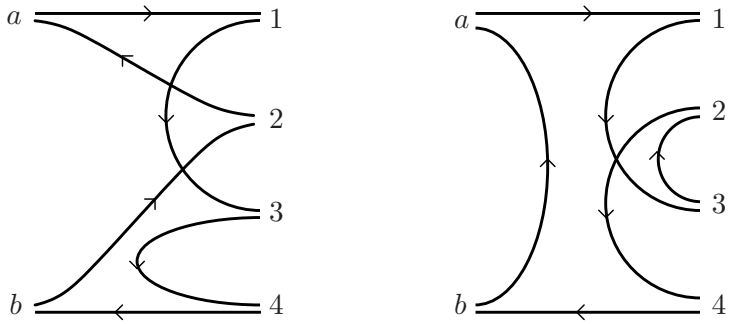

Figure 1. Examples of a colour flow (left) which contributes in the limit of wide angle, hard radiation, and (right) a configuration which is suppressed in the same limit. In these diagrams, the final state gluons (on the right of each picture) are ordered according to their rapidity.

those of the shower. Since the emissions of *HEJ* populate all of phase space (in-between in rapidity of the scatterers of flavour f_1 and f_2), we do not want to define specific regions to populate with *HEJ* and with the shower. Rather, we will let both formalisms populate their respective phase spaces, but define a subtraction term for the shower Sudakov, such that double counting is avoided by reducing the probability of a certain emission from the shower by the probability that *HEJ* had already performed the given emission.

A parton shower framework, such as ARIADNE [6], is necessary in order to evolve the partonic state of *HEJ* to the state of hadronisation, primarily by populating the partonic state with further soft and collinear radiation. As the shower, and also the subsequent string hadronization, relies on having well-defined colour connection between partons, we first need to briefly discuss how these are obtained from *HEJ*.

2.1 The colour connections of High Energy Jets

The colour-ordered Parke-Taylor amplitudes [29] for tree-level $gg \to g \cdots g$-scattering allow for a very neat analysis [30, 31] of the dominant colour configurations in the limit of widely separated, hard gluons. The conclusion, as presented in ref. [30, 31], is that the leading contribution in this limit of *Multi-Regge-Kinematics* (*MRK*) is provided by the colour configurations which can be untwisted to two non-crossing ladders, connecting the rapidity-ordered gluons. Figure 1 (left) contains an example of a configuration contributing in the *MRK*-limit, and one (right) which does not. The numbering of the final state partons is according to their rapidity.

The colour connections in figure 1 (left) can be summarised as $a134b2a$, and if the point for particle 2 is moved to the left side of the same plot, then no colour lines cross. This is always possible if in the colour connection string (like $a134b2a$), the particles entering between the two initial state gluons are ordered in rapidity, as in the case of $a134b2a$.

The colour connections in figure 1 (right) can be summarised as $a1324ba$, which contain an un-ordered string between a and b, and as long as rapidity ordering of the particles is reflected in the vertical position of the particles in figure 1 then one cannot avoid cross-

JHEP07(2011)110

ing colour lines by moving the points from the left to the right side of the plot. This configuration is suppressed in the *MRK*-limit.

Furthermore, the study of ref. [30, 31] shows that all the leading configurations each have the same limit in the *MRK*-limit, and indeed lead to the colour traces resulting in a colour factor C_A for every final state gluon. The limit agrees with that predicted by the amplitudes of Fadin-Kuraev-Lipatov (FKL) [25].

When we pass an event from *High Energy Jets* to ARIADNE, we choose a colour configuration at random from the set of colour connections which are leading in the *MRK*-limit, and pass the event using an interface conforming to the *Les Houches accord* [32].

3 The ARIADNE dipole cascade

The ARIADNE program [6] is based on the colour dipole model developed by the Lund group [14–17], where gluon emissions are modelled as coherent radiation from two colour-connected partons. The general idea is best described in e^+e^--annihilation into jets, where the inclusive probability of emitting a gluon from the original $q\bar{q}$-pair is given by the well known matrix element

$$D(x_1, x_3)dx_1dx_3 = \frac{\alpha_s C_F}{2\pi}\frac{x_1^2 + x_3^2}{(1-x_1)(1-x_3)}dx_1dx_3, \tag{3.1}$$

where x_1 and x_3 are the final-state energy fractions of the quark and anti-quark respectively after the emission. A subsequent gluon emission will then come either from the dipole between the quark and the gluon or from the one between the gluon and the anti-quark, with a trivial generalization to further emissions. The splitting function in eq. (3.1) is modified slightly in the case of dipoles between gluons, giving e.g. for a gluon-gluon dipole,

$$D(x_1, x_3)dx_1dx_3 = \frac{\alpha_s N_c}{4\pi}\frac{x_1^3 + x_3^3}{(1-x_1)(1-x_3)}dx_1dx_3. \tag{3.2}$$

We note that in the soft and collinear limits we have e.g. $x_1 \to z$, $x_3 \to 1$ and $dx_3/(1-x_3) \to dQ^2/Q^2$, where z and Q^2 are the standard energy fraction and virtuality splitting variables, which gives

$$D(x_1, x_3)dx_1dx_3 \to \frac{\alpha_s N_c}{4\pi}\frac{1+z^3}{1-z}dz\frac{dQ^2}{Q^2}. \tag{3.3}$$

Since a given gluon splitting gets contributions from two dipoles we obtain

$$D(z, x_3 \to 1)dzdx_3 + D(1-z, x_3 \to 1)dzdx_3 = \frac{\alpha_s N_c}{2\pi}\frac{(1-z(1-z))^2}{z(1-z)}dz\frac{dQ^2}{Q^2}, \tag{3.4}$$

and we recover the standard gluon splitting function.

Subsequent emissions are ordered in a Lorentz-invariant transverse momentum defined as

$$p_\perp^2 = S_{\rm dip}(1-x_1)(1-x_3) = \frac{s_{12}s_{23}}{S_{\rm dip}}, \tag{3.5}$$

JHEP07(2011)110

(where s_{ij} is the squared invariant mass of partons i and j) which, together with a conveniently defined rapidity,

$$y = \frac{1}{2}\ln\frac{1-x_1}{1-x_3} = \frac{1}{2}\ln\frac{s_{23}}{s_{12}}, \tag{3.6}$$

results in a dipole splitting function which can be approximated by

$$D(p_\perp^2, y)dp_\perp^2 dy \propto \frac{dp_\perp^2}{p_\perp^2}dy. \tag{3.7}$$

The emissions are then made exclusive by introducing no-emission probabilities, or Sudakov form factors, giving the probability that there were no emissions beteen two scales,

$$\Delta(p_{\perp 1}^2, p_{\perp 2}^2) = \exp\left(-\int_{p_{\perp 1}^2}^{p_{\perp 2}^2} dp_\perp^2 \int dy D(p_\perp^2, y)\right) \tag{3.8}$$

giving rise to the standard (next-to-leading) logarithmic resummation of soft and collinear divergences.

In the final state radiation, Ariadne also includes the $g \to q\bar{q}$ splitting, but in this paper we will only concern ourselves with gluon emissions and we will therefore not go into further details.

Ariadne has a fairly unique way of handling radiation in collisions where there are incoming hadrons. In a normal parton shower one would apply a backwards evolution of initial-state splittings, and in more recent dipole shower implementations such as those in Pythia [1] and Sherpa [4], dipoles are defined between incoming and outgoing partons in the hard interaction. The Ariadne program, in contrast, uses the so-called Soft Radiation Model [16], where there are dipoles between the hadron remnants and the partons from the hard interactions.

Here we will rely on the *HEJ* program to generate the initial-state emissions, and we will therefore not go into details of this Soft Radiation Model. Instead we will go back to the dipole splitting function in eq. (3.7) to see how it relates to the matrix elements generated in *HEJ*.

The standard $g \to gg$ splitting function can be derived from ratios of matrix elements (see e.g. chapter 5 in [33]) as

$$d\sigma_{n+1} = \frac{|\mathcal{M}_{n+1}|^2}{|\mathcal{M}_n|^2}\frac{dk_\perp^2 dz}{16\pi^2}d\sigma_n \approx \frac{\alpha_s}{2\pi}P_{gg}(z)\frac{dk_\perp^2}{k_\perp^2}dz d\sigma_n. \tag{3.9}$$

Looking at the dipole splitting function in eq. (3.7), we can associate the emitted gluon to one or the other emitter, depending on which is closer. We can define e.g. $1-z = x_1/(2-x_3)$ and in the limit where parton 3 retains most of its energy we have $dy \approx dz/z$ giving in the end

$$D(p_\perp^2, y) \approx \frac{z}{16\pi^2}\frac{|\mathcal{M}_{n+1}|^2}{|\mathcal{M}_n|^2}. \tag{3.10}$$

This relates the matrix elements to splitting functions, and we will utilise this to define a subtraction term for the shower, based on the matrix elements used in *HEJ*. With this we can proceed with subtracting the radiation probabilities arising in *HEJ* from the Ariadne dipole splittings.

JHEP07(2011)110

4 The subtracted shower

The idea for combining the all-order resummations of *HEJ* and ARIADNE is to first let *HEJ* generate an event according to eq. (2.6), and then let ARIADNE shower these events using a splitting function, which has been modified to subtract the effects of the resummation already included in *HEJ*.

The events from *HEJ* will consist of parton configurations where the two partons extremal in rapidity are required to be members of hard jets (where the scale of hardness is chosen in the analysis) with absolute rapidities less than a cutoff $y_{\max}$ of, say, 5.5. The minimum transverse momenta of these extremal partons can be required to be larger than a scale not much smaller than the jet scale used in the analysis [20]. The phase space in-between these two extremal partons is populated by gluons with transverse momenta above some small cut-off λ (of order 1 GeV), below which a subtraction is applied, in order to organise the cancellation of IR divergences between real and virtual corrections. The *HEJ* events therefore consist of partons of any transverse momentum, and with absolute rapidities less than $y_{\max}$, with the transverse momentum of the two extremal partons larger than the minimum jet transverse scale.

These events are then given to ARIADNE. When ARIADNE performs a trial emission, we subtract from the ARIADNE splitting function the effective splitting function as obtained from *HEJ* for the one extra ARIADNE-emission, as indicated in eq. (3.10)

$$D_{\text{subt}}(p_\perp^2, y) = \frac{z}{16\pi^2} \frac{|\mathcal{M}_{n+1}^{\text{t}}|^2}{|\mathcal{M}_n^{\text{t}}|^2}, \tag{4.1}$$

where the matrix elements are evaluated using the tree-level *HEJ*-formalism of eq. (2.1) (with matching to high-multiplicity full tree-level matrix element, if appropriate). The ratio of the square of matrix elements in eq. (4.1) is given by the factors included in the brackets on the last line of eq. (2.1) — up to the effects of the momentum reshuffling in order to keep the incoming momenta on-shell after the trial emission of the shower (see below). However, in order to take properly into account the effects of the reshuffling, we evaluate the full matrix element (not just the extra factors of $V^\mu V_\mu$) on the respective momenta. The square of the matrix elements is Lorentz-invariant, and the value of z is retained from ARIADNE in the proper dipole frame. This method therefore avoids the need for any Jacobians from a change of reference system.

The n-particle configuration is the original *HEJ*-event, and the ARIADNE trial emission is added to the final state configuration for the evaluation of the matrix element for the $n+1$-particle configuration with a *recoil strategy*, which keeps the incoming partons with zero transverse momentum:

1. The transverse momentum of the trial emission is subtracted from the other final state partons, with the subtraction distributed proportional to the transverse momentum of each parton.

2. The new energy and longitudinal momentum of each parton is defined to keep fixed the rapidity of each of the original partons.

JHEP07(2011)110

Various algorithms were devised for dividing the subtraction of the momentum of the trial emission onto the original *HEJ* partons, each giving very similar results for all the distributions and observables tested. We also tested the subtraction using both the tree-level and the fully regulated formalism for *HEJ*, and the differences are minimal (as expected, since the difference is higher order effects). We therefore choose to use just the tree-level matrix elements, since they evaluate slightly faster (and one avoids complications from the reshuffling moving momenta across the regulating parameter λ).

No subtraction is applied if the ARIADNE trial emission is outside the phase space where *HEJ* would emit gluons, e.g. if the trial emission would result in a configuration where the most forward or backward gluon is softer than the jet scale. This region of emissions collinear to the incoming beam is a domain which is populated purely by the shower.

The described procedure ensures that all the emissions performed by ARIADNE have been properly subtracted to avoid double-counting. But it should also be noted that the veto algorithm[2] used to order the emissions in ARIADNE, automatically ensures that only the subtracted splitting kernel is exponentiated in the Sudakov form factors.

The ordering of emissions in (invariant) transverse momentum in ARIADNE is of some concern. As *HEJ* produces also some very soft gluons ($\sim 1\,\text{GeV}$), there may arise situations where a soft gluon ends up fairly close to a hard one. In this situation ARIADNE would normally first emit some hard, collinearly enhanced, emissions before the softer ones, but now, the dipole between the soft and hard gluon from *HEJ* becomes too small to allow the full range of collinearly-enhanced radiation. The effect is that the very hard jets in our matching procedure will become a bit too narrow. This issue will be discussed further when we look at the resulting jet shapes in the next section.

4.1 The algorithm

What follows here is a step-by-step description of the algorithm as implemented in the *HEJ*/ARIADNE interface.

1. Generate a partonic state with *HEJ*, using a given cutoff in transverse momentum for the extremal partons, and a small transverse momentum cutoff for soft gluons.

2. This state is then sent via PYTHIA to ARIADNE using the Les Houches interface.

3. ARIADNE then sets up its internal dipole event record and starts the dipole cascade starting from a scale given by the largest transverse momentum of any of the *HEJ* partons.

4. For each potential emission in the dipole cascade, check whether it corresponds to something that could have been produced by *HEJ*, i.e. a gluon emission with a rapidity between the two extremal jets. If this is the case:

   - Calculate the kinematics of the gluon and the approximate ratio of matrix elements corresponding to the splitting function used $r_A = |\mathcal{M}_{n+1}|^2 / |\mathcal{M}_n|^2$ according to eq. (3.10).

[2] See e.g. the description of the veto algorithm in the appendix of [34].

JHEP07(2011)110

- This gluon is then sent to *HEJ* using a call-back function where it is inserted in the original partonic state and calculate the ratio of the corresponding matrix element and the original matrix element, $r_H = \left|\mathcal{M}^t_{n+1}\right|^2 / \left|\mathcal{M}^t_n\right|^2$.
- Veto the emission with probability r_h/r_a. This is equivalent to using the subtracted splitting function $D(p_\perp^2, y) - D_{\text{subt}}(p_\perp^2, y)$ in the shower. In addition as this is done inside the veto algorithm, it is the subtracted splitting function which is resummed in the Sudakov form factor.

If the emission is outside the extremal jets, it is kept only if it has a transverse momentum below the cutoff for extremal jets. Furthermore if the emission is a final-state splitting of a gluon into a $q\bar{q}$ pair, it is simply kept as such emissions cannot be produced by *HEJ*. Note also that any gluon emission with a transverse momentum below the phase space slicing parameter λ in *HEJ* will be kept.

5. After the dipole cascade in Ariadne, the partonic final state is hadronized by Pythia, where also the decay of unstable hadrons is performed.

A few notes are in order.

- First it is clear that we avoid double-counting all over phase space. For each emission in the shower, only those which could not have been produced in *HEJ* are kept without change. For those which do correspond to a *HEJ* emission, the corresponding emission probability is subtracted, basically only retaining the collinear pole, while the soft gluons (above the *HEJ* cutoff) are effectively vetoed by the same subtraction algorithm.

- The emissions which are affected by the Soft Radiation Model in Ariadne are those related to dipoles connecting the proton remnants, and these will give gluons outside the extremal jets, and are therefore forced to be below the extremal jet cut. Hence, possible effects of the unconventional treatment of initial state radiation in Ariadne are minimized, and will not lead to extra jets.

- It can be argued that if a gluon emission which is accepted in Ariadne corresponds to a partonic configuration which is not possible to produce by *HEJ*, further emissions from the dipoles connected to this gluon should be unrestricted. Clearly if the gluon was collinear to a *HEJ*-jet, the emissions from the dipole between that jet and the gluon should not be subtracted. On the other hand, emissions from the other dipole should still be subtracted, and the subtraction in the first dipole should be small since it would always correspond to collinear emission. We have tried two scenaria: one where all emissions are subtracted, and one where only emissions from dipoles between original *HEJ* partons are subtracted (this is the default). The differences turned out to be almost negligible.

JHEP07(2011)110

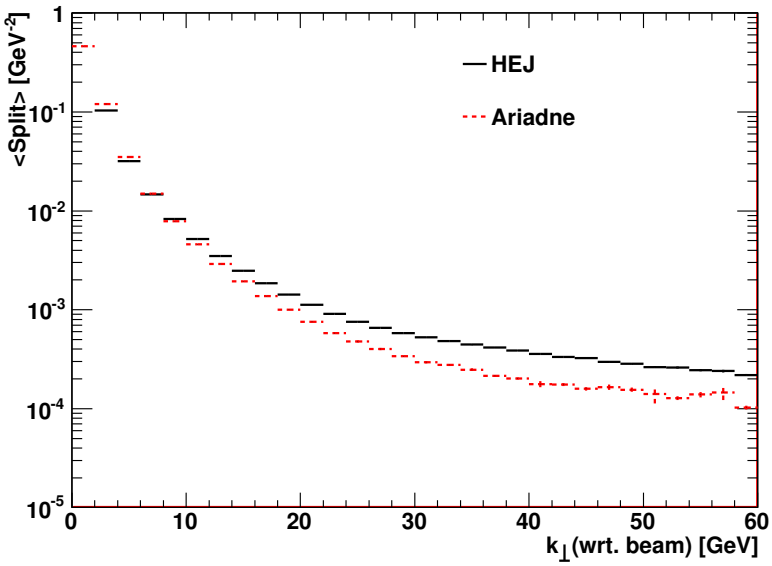

Figure 2. The average value of D/z as a function of the transverse momentum of the trail splitting, for the subset of wide-angle emissions discussed in the text. Hard, wide-angle emissions from Ariadne are (on average) vetoed, since the effective splitting function from *HEJ* is (on average) larger than that from Ariadne.

5 Results

In this section we compare first the effective splitting function from *HEJ* with that of Ariadne, in both the soft and the collinear regions. We then study in details the effects of the shower on a sample event-configuration from *HEJ*, before moving on to a study of the resulting shower profiles, which are compared to ATLAS data. Finally, we discuss the impact of the shower on a few observables discussed in e.g. ref. [20, 35–37], which are sensitive to the description of hard, radiative corrections.

5.1 Comparison of splitting functions

In figure 2 we compare the average value of the splitting functions D/z calculated in Ariadne and with *HEJ* (eq. (4.1)), after division with α_s (to remove the effects of a different evaluation of α_s in Ariadne and *HEJ*), as a function of the transverse momentum of the trial emission. The average is over each bin in the distribution, for an unweighted HEJ event sample of 26 GeV dijets, where at least one reconstructed jet above 30 GeV is required in the post-shower analysis. We have used only the subset of Ariadne trial splittings where the original dipole consists of partons from *HEJ*, and where the trial splitting is at least a distance $R = 0.5$ away from any of the original *HEJ* partons. This is to test only the soft (but not collinear) description in the two frameworks. Generally, the effective splitting functions for wide-angle emissions are quite similar in *HEJ* and Ariadne. However, we see that, on average, the Ariadne splitting function is larger than the effective splitting function from *HEJ* only for emissions of transverse momenta less than about 10 GeV, and

JHEP07(2011)110

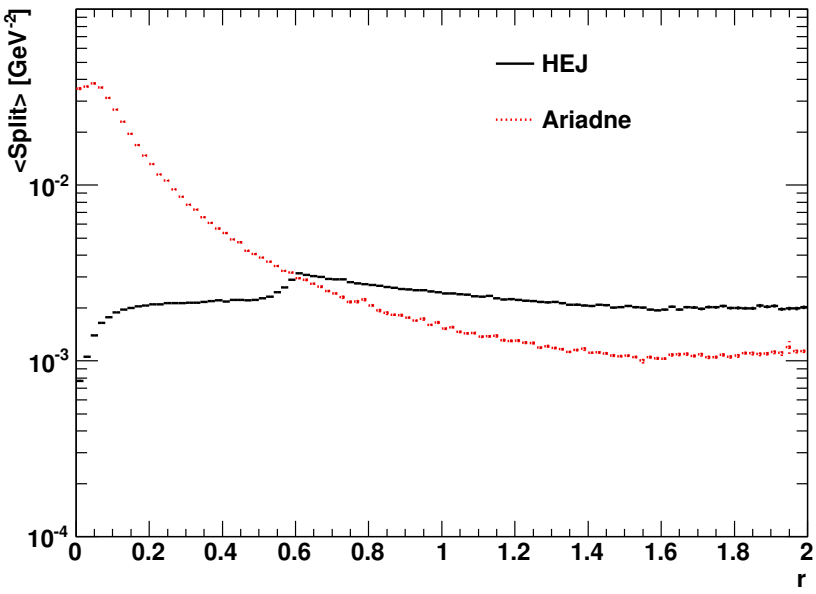

Figure 3. The average value of D/z for trial splittings, as a function of the distance r from the *HEJ* partons, for emissions with transverse momentum greater than 10 GeV. In the collinear region, the ARIADNEsplitting function is much larger than the subtraction from *HEJ*, whereas *HEJ* dominates at larger values of r.

then only by a small amount. This means that effectively, wide-angle emissions harder than about 10 GeV are automatically vetoed in the subtraction mechanism, since the probability for emissions is larger in *HEJ* than in ARIADNE.

We see by comparing the explicit numbers that the *HEJ* splitting function (after division by α_s) tends to $\frac{C_A}{\pi k_\perp^2}$ in the MRK region of semi-hard, wide-angle emissions. This is the result of the full tree-level QCD (and the pure BFKL formalism).

In figure 3 we compare the average value of D/z in ARIADNE and that arising from *HEJ* for a sample of ARIADNE trial emissions (again from original *HEJ* partons) of harder than 10 GeV in transverse momentum, as a function of the distance r (in (rapidity,ϕ)) to the nearest *HEJ* parton. Here we see that at small r, the ARIADNE splitting function is an order of magnitude larger than the subtraction term from *HEJ*. The *HEJ* subtraction term is (on average) larger than the (average) ARIADNE splitting function only for $r > 0.6$, which in this case was also chosen as the jet size parameter in the anti-kt jet clustering. The change in behaviour for the effective *HEJ* splitting function at the jet-size parameter is because of the use of two different effective emission vertices, depending on whether or not the additional *HEJ*-emissions are collinear to the partons extremal in rapidity.

5.2 The description of jet structure

Based on the analysis of the previous subsection, one would expect that the effect of the ARIADNE showering of the *HEJ* events would be to radiate mostly in the immediate sur-

JHEP07(2011)110

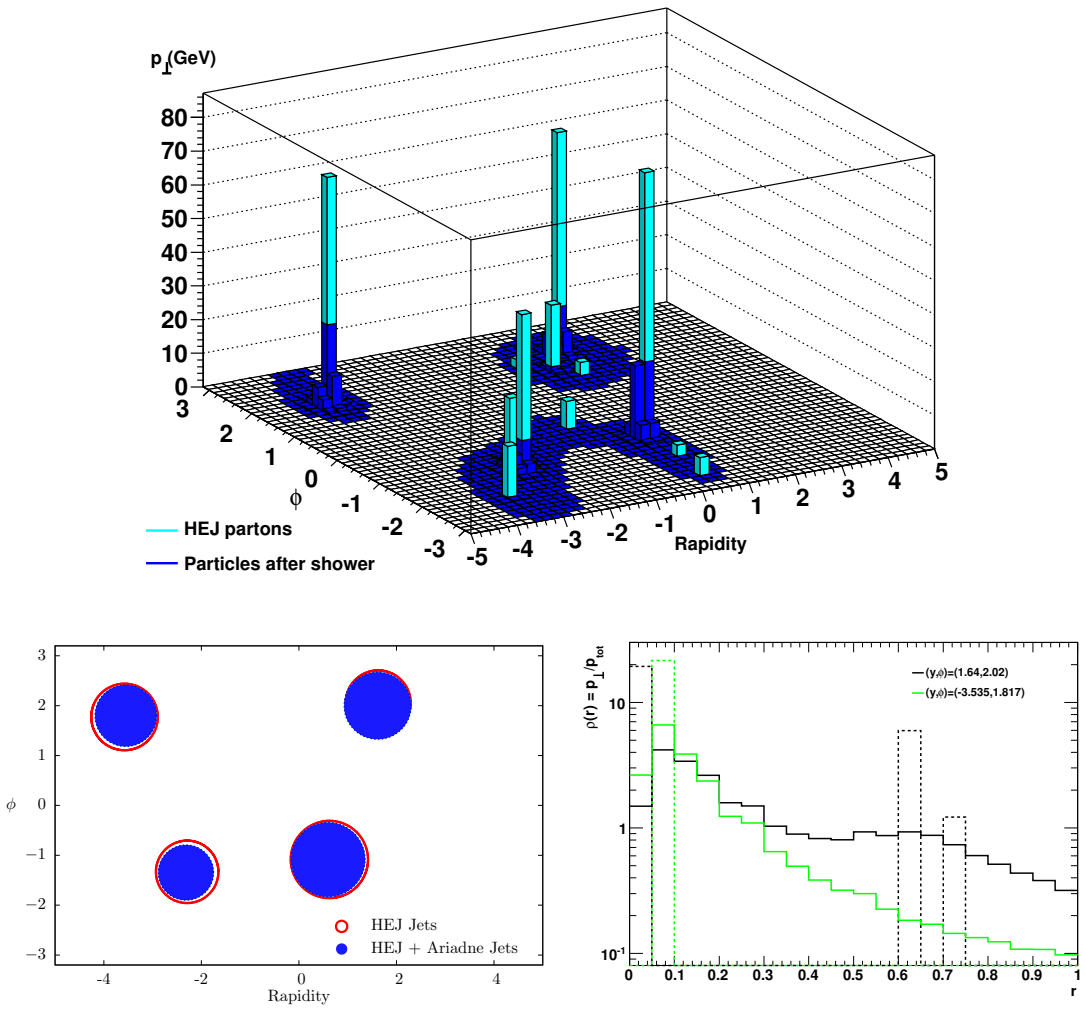

Figure 4. Top: A Lego®-plot of the momentum configuration from HEJ, and the average outcome from 10000 showers of the same HEJ-event. Bottom Left: the 4 hard ($p_\perp > 60\,\text{GeV}$) jets resulting from the jet clustering, before and after the showering. The radii of the circles are proportional to the momentum of the jet. Bottom right: The shower profile of two of the jets, as a function of $r = \sqrt{\Delta y^2 + \Delta\phi^2}$. The dotted lines correspond to the initial partons in each case.

roundings of the existing *HEJ* partons, whereas hard wide-angle emissions from Ariadne should be suppressed.

Figure 4 illustrates the effects of the shower on a sample event from *HEJ*, where the average outcome of 10,000 showers is plotted along with the initial partons. The top Lego plot illustrates clearly the smearing effect of the shower. The effect on the momentum of the reconstructed hard jets (defined with the anti-$k_\perp$ algorithm and $R = 0.6$ and with a transverse momentum larger than 30 GeV) is shown in the bottom left plot, where the radii of the circles is proportional to the momentum of the reconstructed jets. After showering, the jets move only a modest amount in (y, ϕ) and there is only a small change in the

JHEP07(2011)110

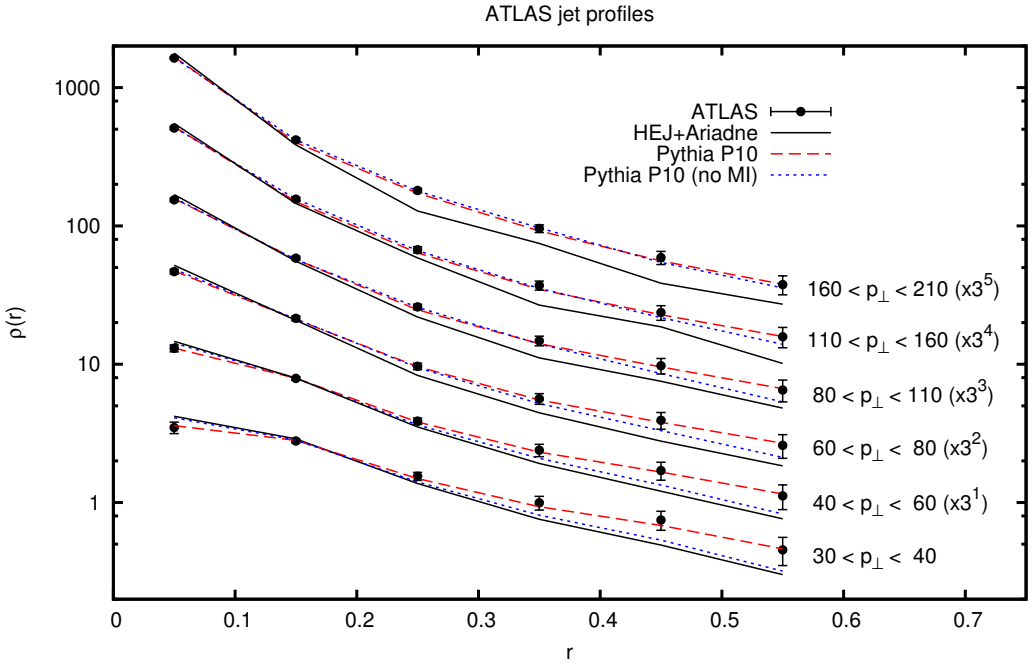

Figure 5. Jet profiles as measured by ATLAS [39] for different bins of jet transvese momenta (in GeV) compared with our results (for $\lambda = 2\,\text{GeV}$) (full lines). Also shown are the results from Pythia Perugia 10 tune with (dashed) and without (dotted) multiple interactions.

momentum. In this particular sample event, the momenta of three of the jets decreases slightly (from {64, 68, 79} GeV to {57, 63, 76} GeV respectively) while the momentum of the other one increases very slightly from 67 GeV to 69 GeV. Further details can be seen in the jet profile plot in the bottom right of figure 4, where the variable plotted is the fraction of the jet's transverse momentum found at a radius r from the jet center:

$$\rho(r) = \frac{1}{p_\perp(R)} \frac{dp_\perp(r)}{dr}, \tag{5.1}$$

where $p_\perp(r)$ is the summed transverse momentum in bins of radius r and R is the jet radius used in the anti-$k_\perp$ algorithm [38].

In figure 5 we present our fully simulated pure QCD inclusive one-jet events (requiring at least two jets of 26 GeV from HEJ, at least one 30 GeV jet after showering) compared to a recent measurement of jet shapes by the ATLAS collaboration [39]. Note that our program does not include any underlying event simulations. We therefore also compare our results with a recent tuning of the Pythia program [40] (Perugia 10 [41]) with and without multiple interactions to estimate such effects. As expected, the underlying event mainly contributes to jets with small transverse momenta in the outskirts of the jets.

We find that our jets are very similar to the Pythia ones (without multiple interactions) for small transverse momenta, which is a good indication that our matching works as expected. However, at larger $p_\perp$ our jets seem to be a bit too narrow as compared to data and Pythia. The reason for this is the very soft gluons fairly close to the hard ones,

JHEP07(2011)110

which are included in the *HEJ* resummation. Such situations result in dipole masses which are too small to allow for enough radiation from the hard gluons within Ariadne.

The problem is that the cascade in Ariadne becomes somewhat un-ordered — the soft gluons should normally be radiated *after* the harder collinear ones as noted in the previous section. This is a problem also in other matching procedures, as noted in [42], especially for the so-called MLM [7, 43] and PseudoJet [44] algorithms. Indeed, in [39] the ATLAS collaboration see a tendency in the Alpgen generator, which uses MLM-merging, to produce too narrow jets at large transverse momenta.

We have here run with a lower cutoff (or regularisation parameter) of the transverse momentum in *HEJ* of 2 GeV, and we have noted that the effect is enhanced if this cutoff is lowered further. Increasing the regularisation parameter further will lead to unacceptably large cancellations between positive and negative weight events. Negative events do not arise in *HEJ* when the regularisation parameter is allowed to be much smaller. To increase the cutoff above 2 GeV is therefore numerically unacceptable, and in any case it would only reduce the effect, not remove it completely.

One could debate whether the subtraction should be applied to *all* Ariadne trial emissions, or only to emissions from Ariadne dipoles made up of partons from *HEJ*. In practice this makes very little difference to the results — certainly, the difference between the two choices are inseparable when presented as in figure 5 (and figures 6–7). We therefore choose to apply the subtraction only in the first emission, in order to limit the amount of momentum reshuffling performed.

5.3 Impact on multi-jet observables

Finally, we are ready to study the impact on a few observables of the addition of a shower to the resummation of *HEJ*. We choose to do so for the observables from a study by ATLAS [45], for which the prediction from *HEJ* were presented in ref. [20]. We do not here present a full analysis of the uncertainties from scale and pdf-variation, as performed in ref. [20], but choose to use as factorisation and renormalisation scale the maximum transverse momentum of any jet, and include the β_0 log-terms, as discussed in ref. [20, 46, 47].

In figure 6 we compare the average number of jets in a dijet-sample (anti-kt, $R = 0.6$) with a transverse momentum greater than 30 GeV (and rapidity less than 4.5) as a function of the rapidity difference between the most forward and backward hard jet. These two jets are furthermore required to have an average transverse momentum greater than 60 GeV. The black line is the partonic prediction from *HEJ* (based on just the FKL-configurations discussed in the current paper). The blue dashed line is obtained after the further shower and hadronisation by Ariadne. The changes (due to the showering) in the number of hard jets is very small indeed, but increasing in significance with the rapidity span and the average number of jets. At a rapidity span of 6 units, the showering and hadronisation leads to a reduction in the average number of hard jets from roughly 3.6 to slightly above 3.5. For small rapidity spans ($\Delta y < 2$), the showering and hadronisation leads to a minute increase in the average number of hard jets, whereas for larger rapidity spans the effect is a larger decrease.

JHEP07(2011)110

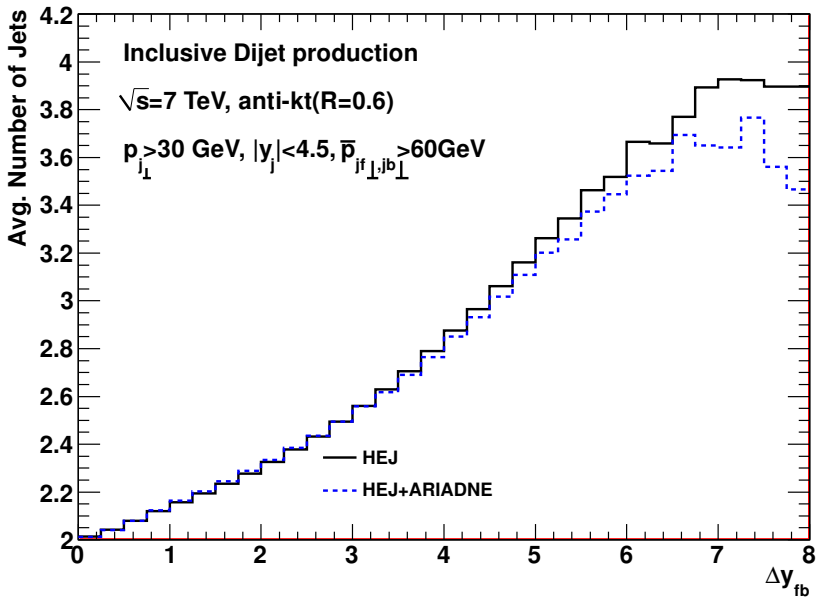

Figure 6. The average number of jets vs. the rapidity difference between the most forward/backward jet as obtained with HEJ, and with HEJ+ARIADNE. The total effects of shower and hadronisation on this observable are minor.

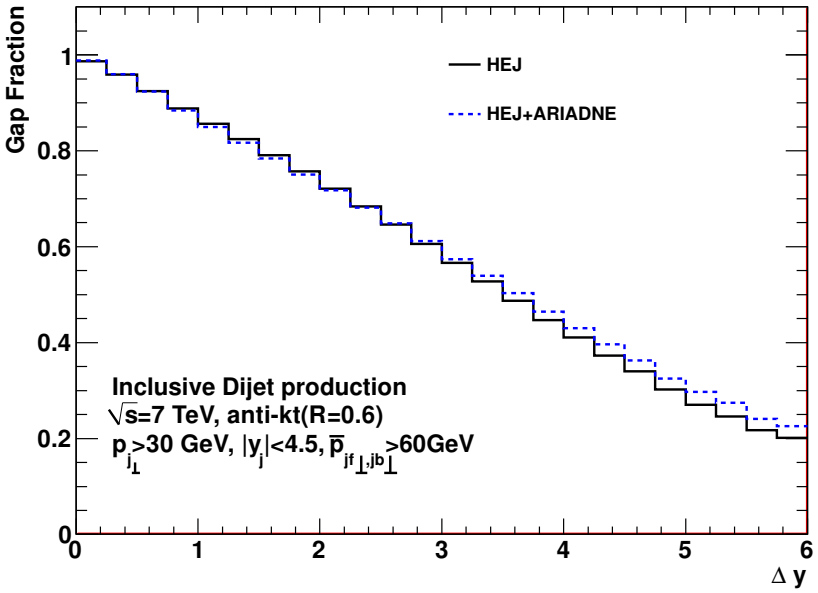

Figure 7. The gap fraction (exclusive dijet over inclusive dijet rate) as a function of the rapidity span between the most forward/backward hard jet, as obtained with HEJ, and with HEJ+ARIADNE. The total effects of shower and hadronisation on this observable are minor.

JHEP07(2011)110

The trend and small effect is found again in the prediction of the *gap fraction* in figure 7, defined here as the exclusive dijet rate over the inclusive dijet rate, as a function of the rapidity span between the most forward/backward pair of hard jets ($p_\perp > 30\,\text{GeV}$). The effects seen in figure 6 are repeated here — for small rapidity spans ($\Delta y < 2$), the showering and hadronisation leads to a minute decrease in the gap fraction, but for larger rapidity spans, the effect is a small increase.

6 Outlook

We have here presented a procedure for obtaining exclusive hadronic final states within the framework of *HEJ*, describing jet production in high-energy hadronic collisions. To do this we have developed a new kind of matching scheme dealing with two separate all-order summations, where the hard jets (and soft contributions) are first generated in *HEJ*, followed by a final-state shower dressing up the jets with further subtracted soft and collinear radiation. Double-counting is avoided by carefully removing the appropriate soft divergences in the parton shower in a way such that the collinear divergences are still correctly exponentiated.

We have validated our procedure both technically, by making sure that the subtracted splitting functions look reasonable, and also by comparing the resulting jet shapes with recent measurements by the ATLAS experiment. For the latter we find very good agreement with data. We have also shown that previous predictions published for the *HEJ* model at parton level are fairly insensitive to the addition of parton showers and hadronization for reasonable choices of jet definitions.

We have, however, found that our results are somewhat sensitive to the very soft gluon emissions also included in *HEJ*. The reason can be understood from the fact that Ariadne is forced to work in an un-ordered way. Some soft emissions from *HEJ*, would normally be emitted by Ariadne after the emission in the collinear region. This indirectly reduces the phase space available for collinear emissions, giving jets which are a bit too narrow, especially at high transverse momenta. The situation is similar to the problems found in [42] when investigating the so-called MLM [7, 43] and PseudoJet [44] merging procedures.

In the future we will investigate different ways of solving this problem, and we have already identified two different solutions. One is based on the CKKW(-L) [5, 48] merging procedure. Here the states produced by *HEJ* would first be reweighted by Sudakov form factors produced by the properly subtracted parton shower, whereafter the shower can be added in the same way as presented in this article. Here we plan to use a recent CKKW-L implementation in the Pythia generator [49], which will also allow us to add underlying events from the multiple-interaction model in Pythia.

Another option we will pursue is related to the concept of *primary* or *back-bone* gluons introduced in [50] and [51]. There it is found that the main real-emission contribution to the cross section according to BFKL is given by gluons which are ordered in both positive and negative light-cone momenta, while other emissions can be conveniently summed over. In our case that would mean that soft gluons produced in *HEJ* that are not ordered in this fashion would simply be removed in a kind of *post-factum* resummation. After that

JHEP07(2011)110

the parton shower, this time *unsubtracted*, can be applied with a simple phase space veto, allowing only gluons emissions which are un-ordered in light-cone momenta, in the same way as has been done in [52] and [53].

Nevertheless, we have found that the effects of the non-ordering of the parton shower are small, and the current implementation is therefore an important step forward in the description of multi-jet events in hadronic collisions. This is the first framework that will properly simulate complete multi-jet final states with proper resummation of also semi-hard emissions at high energies, and will provide an important alternative to the conventional event generator approaches, which are all based on DGLAP resummation only.

Acknowledgments

We would like to thank Frank Krauss, Gavin Salam, Peter Richardson, Mike Seymour and Peter Z. Skands for discussions on matching to parton showers.

Work supported in part by the EU Marie Curie RTN MCnet (MRTN-CT-2006-035606), the Swedish research council (contracts 621-2008-4252 and 621-2009-4076) and the UK Science and Technology Facilities Council (STFC).

L.L. gratefully acknowledges the hospitality of the CERN theory unit. JRA also acknowledges the support of CERN TH during various stages of this work.

References

[1] T. Sjöstrand, S. Mrenna and P.Z. Skands, *A brief introduction to PYTHIA* 8.1, *Comput. Phys. Commun.* **178** (2008) 852 [arXiv:0710.3820] [SPIRES].

[2] G. Marchesini and B.R. Webber, *Monte Carlo simulation of general hard processes with coherent QCD radiation*, *Nucl. Phys.* **B 310** (1988) 461 [SPIRES].

[3] M. Bähr et al., *HERWIG++ physics and manual*, *Eur. Phys. J.* **C 58** (2008) 639 [arXiv:0803.0883] [SPIRES].

[4] T. Gleisberg et al., *Event generation with SHERPA* 1.1, *JHEP* **02** (2009) 007 [arXiv:0811.4622] [SPIRES].

[5] S. Catani, F. Krauss, R. Kuhn and B.R. Webber, *QCD matrix elements + parton showers*, *JHEP* **11** (2001) 063 [hep-ph/0109231] [SPIRES].

[6] L. Lönnblad, *ARIADNE version* 4*: a program for simulation of QCD cascades implementing the color dipole model*, *Comput. Phys. Commun.* **71** (1992) 15 [SPIRES].

[7] M.L. Mangano, M. Moretti and R. Pittau, *Multijet matrix elements and shower evolution in hadronic collisions:* $Wb\bar{b} + n$ *jets as a case study*, *Nucl. Phys.* **B 632** (2002) 343 [hep-ph/0108069] [SPIRES].

[8] H. Jung and G.P. Salam, *Hadronic final state predictions from CCFM: the hadron-level Monte Carlo generator CASCADE*, *Eur. Phys. J.* **C 19** (2001) 351 [hep-ph/0012143] [SPIRES].

JHEP07(2011)110

[9] H. Jung et al., *The CCFM Monte Carlo generator CASCADE* 2.2.0, *Eur. Phys. J.* **C 70** (2010) 1237 [arXiv:1008.0152] [SPIRES].

[10] M. Ciafaloni, *Coherence effects in initial jets at small Q^2/s*, *Nucl. Phys.* **B 296** (1988) 49 [SPIRES].

[11] S. Catani, F. Fiorani and G. Marchesini, *QCD coherence in initial state radiation*, *Phys. Lett.* **B 234** (1990) 339 [SPIRES].

[12] S. Catani, F. Fiorani and G. Marchesini, *Small x behavior of initial state radiation in perturbative QCD*, *Nucl. Phys.* **B 336** (1990) 18 [SPIRES].

[13] G. Marchesini, *QCD coherence in the structure function and associated distributions at small x*, *Nucl. Phys.* **B 445** (1995) 49 [hep-ph/9412327] [SPIRES].

[14] G. Gustafson, *Dual description of a confined color field*, *Phys. Lett.* **B 175** (1986) 453 [SPIRES].

[15] G. Gustafson and U. Pettersson, *Dipole formulation of QCD cascades*, *Nucl. Phys.* **B 306** (1988) 746 [SPIRES].

[16] B. Andersson, G. Gustafson, L. Lönnblad and U. Pettersson, *Coherence effects in deep inelastic scattering*, *Z. Phys.* **C 43** (1989) 625 [SPIRES].

[17] L. Lönnblad, *Rapidity gaps and other final state properties in the color dipole model for deep inelastic scattering*, *Z. Phys.* **C 65** (1995) 285 [SPIRES].

[18] J.R. Andersen and J.M. Smillie, *Constructing all-order corrections to multi-jet rates*, *JHEP* **01** (2010) 039 [arXiv:0908.2786] [SPIRES].

[19] J.R. Andersen and J.M. Smillie, *The factorisation of the t-channel pole in quark-gluon scattering*, *Phys. Rev.* **D 81** (2010) 114021 [arXiv:0910.5113] [SPIRES].

[20] J.R. Andersen and J.M. Smillie, *Multiple jets at the LHC with high energy jets*, *JHEP* **06** (2011) 010 [arXiv:1101.5394] [SPIRES].

[21] W.T. Giele, D.A. Kosower and P.Z. Skands, *A simple shower and matching algorithm*, *Phys. Rev.* **D 78** (2008) 014026 [arXiv:0707.3652] [SPIRES].

[22] T. Sjöstrand et al., *High-energy physics event generation with PYTHIA* 6.1, *Comput. Phys. Commun.* **135** (2001) 238 [hep-ph/0010017] [SPIRES].

[23] T. Sjöstrand, L. Lönnblad, S. Mrenna and P.Z. Skands, *PYTHIA* 6.3 *physics and manual*, hep-ph/0308153 [SPIRES].

[24] V.S. Fadin, E.A. Kuraev and L.N. Lipatov, *On the Pomeranchuk singularity in asymptotically free theories*, *Phys. Lett.* **B 60** (1975) 50 [SPIRES].

[25] E.A. Kuraev, L.N. Lipatov and V.S. Fadin, *Multi-reggeon processes in the Yang-Mills theory*, *Sov. Phys. JETP* **44** (1976) 443 [SPIRES].

[26] E.A. Kuraev, L.N. Lipatov and V.S. Fadin, *The Pomeranchuk singularity in nonabelian gauge theories*, *Sov. Phys. JETP* **45** (1977) 199 [SPIRES].

[27] I.I. Balitsky and L.N. Lipatov, *The Pomeranchuk singularity in quantum chromodynamics*, *Sov. J. Nucl. Phys.* **28** (1978) 822 [SPIRES].

[28] J. Alwall et al., *MadGraph/MadEvent v4: the new web generation*, *JHEP* **09** (2007) 028 [arXiv:0706.2334] [SPIRES].

JHEP07(2011)110

[29] S.J. Parke and T.R. Taylor, *An amplitude for n gluon scattering*, *Phys. Rev. Lett.* **56** (1986) 2459 [SPIRES].

[30] V. Del Duca, *Parke-Taylor amplitudes in the multi-Regge kinematics*, *Phys. Rev.* **D 48** (1993) 5133 [hep-ph/9304259] [SPIRES].

[31] V. Del Duca, *Equivalence of the Parke-Taylor and the Fadin-Kuraev-Lipatov amplitudes in the high-energy limit*, *Phys. Rev.* **D 52** (1995) 1527 [hep-ph/9503340] [SPIRES].

[32] E. Boos et al., *Generic user process interface for event generators*, hep-ph/0109068 [SPIRES].

[33] R.K. Ellis, W.J. Stirling and B.R. Webber, *QCD and collider physics*, Cambridge University Press, Cambridge U.K. (1996).

[34] A. Buckley et al., *General-purpose event generators for LHC physics*, *Phys. Rept.* **504** (2011) 145 [arXiv:1101.2599] [SPIRES].

[35] J.R. Andersen, V. Del Duca and C.D. White, *Higgs boson production in association with multiple hard jets*, *JHEP* **02** (2009) 015 [arXiv:0808.3696] [SPIRES].

[36] J.R. Andersen and W.J. Stirling, *Energy consumption and jet multiplicity from the leading log BFKL evolution*, *JHEP* **02** (2003) 018 [hep-ph/0301081] [SPIRES].

[37] J.R. Andersen and J.M. Smillie, *High energy description of processes with multiple hard jets*, *Nucl. Phys. Proc. Suppl.* **205-206** (2010) 205 [arXiv:1007.4449] [SPIRES].

[38] M. Cacciari, G.P. Salam and G. Soyez, *The anti-k_t jet clustering algorithm*, *JHEP* **04** (2008) 063 [arXiv:0802.1189] [SPIRES].

[39] ATLAS collaboration, G. Aad et al., *Study of jet shapes in inclusive jet production in pp collisions at $\sqrt{s} = 7$ TeV using the ATLAS detector*, *Phys. Rev.* **D 83** (2011) 052003 [arXiv:1101.0070] [SPIRES].

[40] T. Sjöstrand, S. Mrenna and P.Z. Skands, *PYTHIA* 6.4 *physics and manual*, *JHEP* **05** (2006) 026 [hep-ph/0603175] [SPIRES].

[41] P.Z. Skands, *Tuning Monte Carlo generators: the Perugia tunes*, *Phys. Rev.* **D 82** (2010) 074018 [arXiv:1005.3457] [SPIRES].

[42] N. Lavesson and L. Lönnblad, *Merging parton showers and matrix elements — Back to basics*, *JHEP* **04** (2008) 085 [arXiv:0712.2966] [SPIRES].

[43] M. Mangano, *The so-called mlm prescription for me/ps matching*, talk presented at the *Fermilab ME/MC Tuning Workshop*, October 4, Fermilab, U.S.A. (2002), http://www-cpd.fnal.gov/personal/mrenna/tuning/nov2002/mlm.pdf.gz.

[44] S. Mrenna and P. Richardson, *Matching matrix elements and parton showers with HERWIG and PYTHIA*, *JHEP* **05** (2004) 040 [hep-ph/0312274] [SPIRES].

[45] ATLAS collaboration, *Measurement of dijet production with a jet veto in pp collisions at $\sqrt{s} = 7$ TeV using the ATLAS detector*, ATLAS-CONF-2010-085.

[46] J.R. Andersen and A. Sabio Vera, *Solving the BFKL equation in the next-to-leading approximation*, *Phys. Lett.* **B 567** (2003) 116 [hep-ph/0305236] [SPIRES].

[47] J.R. Andersen and A. Sabio Vera, *The gluon Green's function in the BFKL approach at next-to-leading logarithmic accuracy*, *Nucl. Phys.* **B 679** (2004) 345 [hep-ph/0309331] [SPIRES].

JHEP07(2011)110

[48] L. Lönnblad, *Correcting the colour-dipole cascade model with fixed order matrix elements*, *JHEP* **05** (2002) 046 [hep-ph/0112284] [SPIRES].

[49] L. Lönnblad and S. Prestel, *Matching tree-level matrix elements with interleaved showers*, Preprint in preparation.

[50] B. Andersson, G. Gustafson and J. Samuelsson, *The linked dipole chain model for DIS*, *Nucl. Phys.* **B 467** (1996) 443 [SPIRES].

[51] G.P. Salam, *Soft emissions and the equivalence of BFKL and CCFM final states*, *JHEP* **03** (1999) 009 [hep-ph/9902324] [SPIRES].

[52] H. Kharraziha and L. Lönnblad, *The linked dipole chain Monte Carlo*, *JHEP* **03** (1998) 006 [hep-ph/9709424] [SPIRES].

[53] C. Flensburg, G. Gustafson and L. Lönnblad, *Inclusive and exclusive observables from dipoles in high energy collisions*, arXiv:1103.4321 [SPIRES].

JHEP07(2011)110